Journal of Applied Mechanics and Technical Physics, Vol. 50, No. 5, pp. 747–753, 2009

NUMERICAL SIMULATIONS OF GAS-DYNAMIC CONDUCTIVITY OF MICROCHANNELS WITH ALLOWANCE FOR THEIR SURFACE STRUCTURE

A. I. Ukhov,[1] B. T. Porodnov,[1] and S. F. Borisov[2]

UDC 536.244: 533.6.011

The effect of the microchannel surface structure on the free-molecular gas flow is studied by the test-particle method. Simulations are performed for channels whose surface either is obtained by means of statistical modeling or is reconstructed from the data of atomic-force microscopy of real surfaces. Dependences of monochromatic molecular beam scattering on the angle of incidence and the average height of microscopic roughness elements on the surface are considered. It is demonstrated that the method developed allows one to obtain the distribution function for particles reflected from a rough surface and to use it in the boundary conditions in problems of rarefied gas dynamics.

Key words: *rarefied gas flow in microchannels, Monte Carlo test-particle method, gas–surface interaction, scattering indicatrices, atomic-force microscopy.*

Introduction. In solving gas-dynamic problems associated with re-entry of flying vehicles into the upper atmospheric layers or with gas flows in microscale or nanoscale devices, one should take into account the parameters characterizing the structure and chemical composition of the surface. Numerous experimental studies show that the surface structure, its temperature, and other factors exert a significant effect on scattering of rarefied gas molecules and, as a consequence, on the gas-dynamic drag and heat transfer in the gas–solid system [1].

One important component of the model of gas dynamics in external and internal flows are the boundary conditions for the Boltzmann equation, which imply that the distribution function of gas molecules reflected from the surface is available in an analytical form. This function depends on many characteristics of the gas and the surface, and also on thermodynamic parameters of the system as a whole. One factor exerting a significant effect on energy and momentum transfer in the gas–solid system is physical inhomogeneity (roughness) of the surface.

Because of the lack of information about the surface structure and its role in gas–solid interaction, approaches with the use of absolutely smooth surfaces or extremely simple roughness models are usually used [2]. The influence of the surface structure on the free-molecular gas flow in cylindrical channels was studied in experiments [3, 4].

The development of methods of computer modeling and the use of new experimental technologies, in particular, scanning probe microscopy, allow certain progress to be achieved in numerical simulations of gas scattering on rough surfaces and in the description of rarefied gas flows in channels with the surface structure corresponding to conditions of physical experiments [5–7].

The use of atomic force microscopy allows one to obtain high-resolution three-dimensional topograms. The thus-obtained digitized surface is an array whose elements contain the coordinates of each point of the surface of the examined sample. In the present work, we used the coordinates of 160 thousand points on the surface of a 20×20 μm silicon single crystal. In the course of studying the specified rough surface, we determined its basic characteristics. It was found that the distribution of microscopic roughness elements in terms of their height follows the normal distribution law; the average height of the microscopic roughness elements was $\langle Z \rangle = 1.106$ μm, and the root-mean-square deviation was $\sigma = 0.275$ μm.

[1]Ural State Technical University, Ekaterinburg 620002; sanek_uhov@mail.ru. [2]Ural State University, Ekaterinburg 620083. Translated from Prikladnaya Mekhanika i Tekhnicheskaya Fizika, Vol. 50, No. 5, pp. 20–27, September–October, 2009. Original article submitted November 7, 2008.

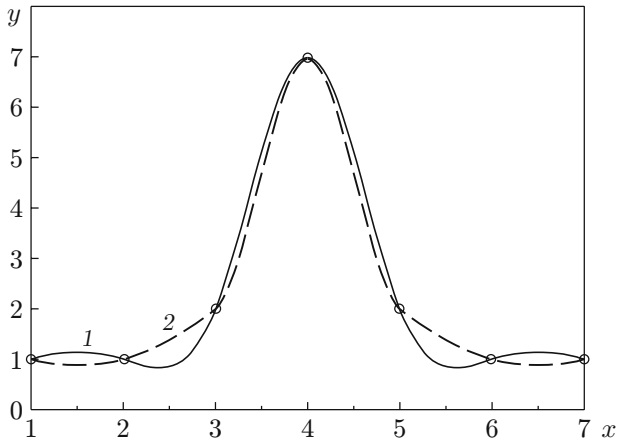

Fig. 1. Cubic spline (1) and Akima spline (2) constructed from identical initial data (points).

Simulation of Surface Structures. Individual roughness elements (peaks) were simulated by statistical methods, which are used for sampling the height R_h and width R_w of the microscopic roughness elements in accordance with the analytical form of the distribution function of their height obtained from the data of atomic-force microscopy.

In simulating the peak shape, we solved the problem of resampling (replenishment) arising in passing from a regular grid with $m_1 \times n_1$ nodes to a grid with $m_2 \times n_2$ nodes. In this case, we have to calculate the values of the function on the new grid, using the values of the function on the regular grid. Thus, the node (2,2) of the 3×3 initial grid is assigned the value R_h, and the values of the remaining nodes of the grid are assumed to be equal to zero. After that, resampling of the initial matrix on a $R_w \times R_w$ grid is performed. The values of the function in the nodes of the new matrix (replenishment problem) can be determined by various methods, for instance, bilinear and bicubic resampling. In the case of bicubic resampling, it is necessary to construct a table of coefficients of a piecewise-linear spline, a cubic spline, or an Akima spline. In the present work, we used the Akima spline chosen because the shape of the resultant peaks is close to the shape observed by atomic-force microscopy of the samples and because the Akima spline is stable to spikes. Note that a common significant drawback of cubic splines is their oscillation in the vicinity of a point substantially different from the neighboring points. Figure 1 shows the cubic spline and the Akima spline constructed on the basis of identical initial data. In contrast to the cubic spline, the Akima spline is seen to be less subjected to the influence of spikes. There are practically no signs of oscillations on the segments adjacent to the spike point, which determined our choice of the spline form for modeling the surface roughness.

At the final stage of modeling, the resultant peak is transferred onto the simulated surface. The use of an additional parameter ρ in surface-structure simulations allows us to specify the distribution density function of roughness elements on the simulated structure by sampling a random quantity R_f. If the sampled value of R_f is smaller than the value of ρ, the peak is transferred onto the surface.

In what follows, two or several surfaces can be combined into one more "complicated" surface. A new surface is formed by means of such a combination based on superposition of structures defined in a certain manner. The coordinate Z_{res} of the height of each point of this surface is determined by means of addition (subtraction) or by means of choosing the maximum (minimum) value of two coordinates of the heights of the points of the initial surfaces:

$$Z_{\text{res}} = \begin{cases} \sum (Z_1 + Z_2), \\ \text{sub}\,(Z_1 - Z_2), \\ \max (Z_1, Z_2), \\ \min (Z_1, Z_2). \end{cases}$$

Using the functions $Z_1 = \sin(x)$ and $Z_2 = 0.3$, we can construct two surface profiles: $Z_{\text{res}} = \max(\sin(x), 0.3)$ or $Z_{\text{res}} = \min(\sin(x), 0.3)$. Assembling different combinations of the functions, changing the function parameters [e.g., the amplitude α or the period β of the function $Z_1 = \alpha \sin(\beta x)$], or using more complicated functions, we can obtain a rather broad range of rough surfaces.

Simulation of Scattering. The simulation is based on scattering of a monochromatic molecular beam on a rough surface whose structure is reconstructed from the data of atomic-force microscopy. For an analytical search for the point of intersection of the particle trajectory, the surface was covered with a triangulation grid. Simulations were performed either by the method of the test particle interacting with the surface at different angles of incidence and a given average height of microscopic roughness elements for two values of the coefficient of diffuse reflection of molecules from the surface element: $\varepsilon = 1$ (completely diffuse reflection) and $\varepsilon = 0$ (completely specular reflection). In these simulations, we studied the effect of the roughness height on scattering of particles by changing the average height of microscopic roughness elements via changing the height factor $H = 0$–5. The value $H = 1$ corresponds to the surface reconstructed from the data obtained by atomic-force microscopy of the experimentally studied sample.

Before simulating the scattering process, we assigned the velocity vector (depending on the angle of incidence) for all particles and their random positions on the plane located above the examined surface parallel to the latter. The point of intersection of the particle trajectory with surface elements is found by the method of "shells" widely used in computer graphics. In this method, the examined surface area is presented in the form of rectangular parallelepipeds with an identical base area and with the height equal to the local maximum height of the roughness element located on this area. Each parallelepiped has a certain set of triangles in the base. If the particle intersects one of the shells (parallelepiped), we consider the possibility of particle intersection only with those triangles that belong to this shell. The use of this method allows the time of searching for the particle trajectory-surface intersection point to be substantially reduced. For this purpose, it is necessary to find the point of intersection of the straight line with the plane constructed in the base of the triangle and then to determine whether the intersection point belongs to this triangle: if the point is inside the triangle, then the particle crossed the surface; if the point is outside the triangle, then the particle did not collide with the surface. Simulation of the particle motion is terminated when the particle leaves the computational domain after its collision with the surface, but the information about the particle velocity components and about the number of particle collisions with the surface is stored. The number of particles within specified angles of reflection from the surface is also determined; this information is further used to construct scattering indicatrices.

Prior to simulations, we performed some test computations, where we considered scattering of particles on an absolutely smooth surface with completely diffuse and completely specular variants of interaction and with the particle incidence angle $\theta_i = 45°$. In the first case, we obtained scattering indicatrices that satisfy the cosine law; in the second case, we obtained a δ-function with the reflection angle $\theta_r = 45°$.

At the first stage of the numerical experiment, we considered completely specular reflection of beam particles from the surface ($\varepsilon = 0$). Simulations were performed for $H = 1$, 2, 3, 4, and 5 and angles of incidence $\theta_i = 0$, 15, 45, and 75°. Figure 2 shows the scattering indicatrices in the plane of incidence of the beam scattered on a "real" surface ($H = 1$) with different angles of incidence θ_i. According to Fig. 2, the angle of reflection θ_r decreases with decreasing angle of incidence θ_i. As the height factor is increased from $H = 1$ to $H = 5$, the scattering indicatrices are seen to change from the lobed shape (at $H = 1$ and 2) to cosine shapes typical for diffuse scattering of particles (at $H > 2$).

At the next stage of the numerical experiment, we considered the case of completely diffuse interaction ($\varepsilon = 1$). We studied the scattering of a molecular beam at angles of incidence $\theta_i = 0$, 15, 45, and 75° on surfaces with the height factor $H = 1$, 3, and 5. Figures 3a to 3d show the distributions of the velocity component v_y obtained for these angles of incidence and the height factor $H = 3$. Figures 3e to 3h show the corresponding indicatrices constructed in the plane of incidence of the beam and the cosine distribution.

It follows from Fig. 3 that the deviation of the resultant curve for the velocity component v_y from the Gaussian distribution decreases as the angle of incidence θ_i is reduced, and the two functions coincide at $\theta_i = 0$. Correspondingly, the indicatrix changes from the lobed shape to the cosine distribution. At $H = 1$, the deviation of the resultant distribution of the velocity component v_y from the Gaussian curve and the slope of the indicatrices are smaller than the corresponding values at $H = 5$. The following explanation can be found for the decrease in the deviation of the distribution of the velocity component v_y from the normal curve and for the decrease in the slope of the scattering indicatrix with decreasing angle of incidence of the molecular beam. If the particles fly at an angle of incidence $\theta_i > 15°$, then some of them are reflected after collisions with the roughness peaks, which affects the shape of the indicatrix and the displacement of the distribution function of the velocity component v_y. If the particle incidence angle is $\theta_i < 15°$, then the first collisions of the particles with the surface occur at a depth greater than

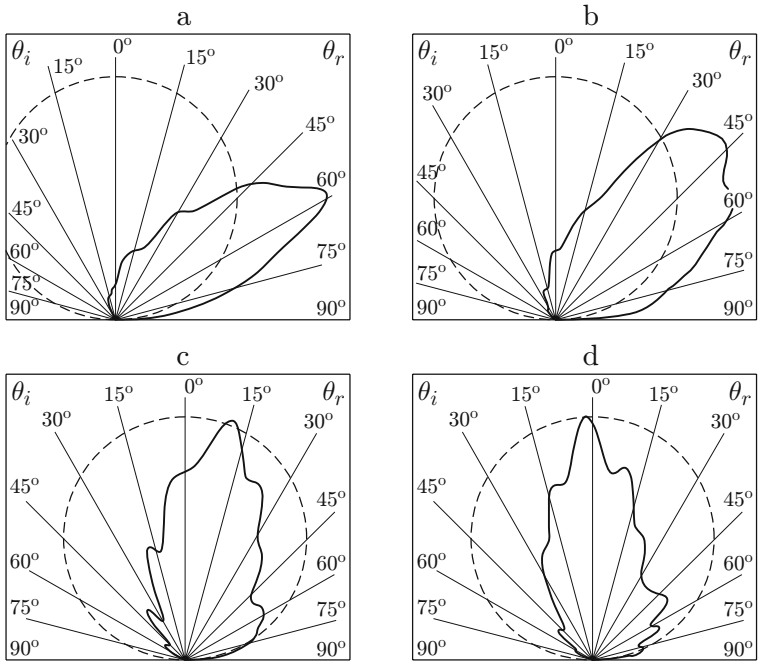

Fig. 2. Scattering indicatrices for particles reflected from the surface ($\varepsilon = 0$) for $H = 1$ and $\theta_i = 75^\circ$ (a), 45° (b), 15° (c), and 0 (d): the dashed curves show the cosine distribution.

that in the previous case. For this reason, the number of reflected particles decreases, and the indicatrix acquires the shape of the cosine distribution. The distribution of the velocity component v_y acquires the same shape as that in the case of diffuse scattering on a smooth surface.

In processing the data of the numerical experiment, we used the method of determining the distribution function of the velocity components of reflected particles, which can be presented as a combination of exponents with the corresponding coefficients:

$$f(v_j) = \sum_{i=1}^{n} h_i \exp\Big(- \frac{(v_j - a_i)^2}{2\sigma_i^2}\Big), \qquad j = x, y, z. \tag{1}$$

Based on the data on the velocity of each particle after its interaction with the surface, the distribution function of the velocity components of reflected particles (1) is sought in an analytical form by determining the values of the coefficients a_i, σ_i, and h_i with the use of the nonlinear least squares technique. Experimental data are described more precisely if the sought function is chosen in such a form. The choice of the value of n determines the accuracy of approximation of experimental data by the empirical formula (1). Using the algorithm of modeling of the specified distribution, we can sample the velocity components of reflected particles with specifying the coefficients h_i, a_i, and σ_i for each particle. The distribution functions obtained can be used for simulating the velocity components of reflected particles for the structure of similar surfaces.

Modeling of Gas Flows in Channels. The surface of the examined channels either was simulated by the above-described technique or was reconstructed from the data of atomic-force microscopy. The channel conductivity (quantity inverse to the particle passage probability) was determined by the test-particle method [8]. The particle passage probability w is equal to the number of particles that passed through the channel to the total number of particles at the channel entrance. A case with completely diffuse interaction ($\varepsilon = 1$) was considered.

In simulations, the channel wall is covered by a triangulation grid. Each triangle in this grid belongs to a certain mini-cylinder; the set of these mini-cylinders forms the channel wall. To seek for the point of intersection with the channel wall, the particle trajectory is divided at each stage of its motion into segments of identical length. Then, the point of the beginning of each segment is checked in terms of its belonging to one of the mini-cylinders. In what follows, only the triangles belonging to crossed cylinders are considered for determining the point of intersection of the particle trajectory with the channel wall. If the trajectory intersects the channel surface at several places, it

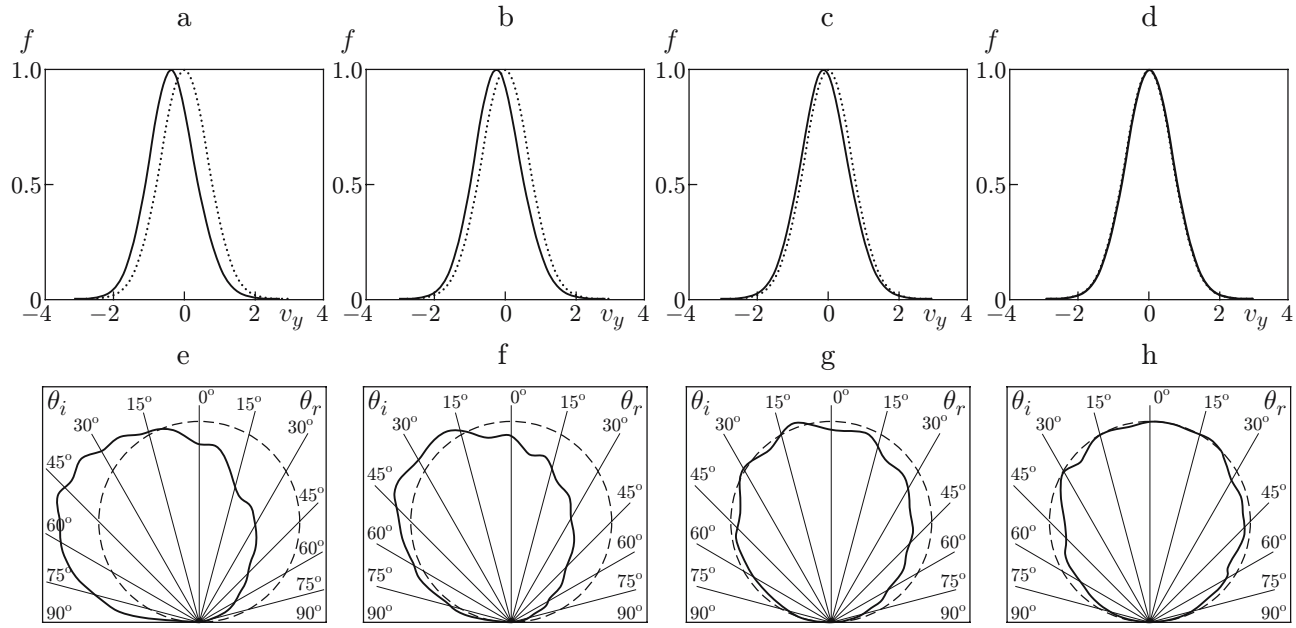

Fig. 3. Distributions of the velocity component v_y of particles reflected from the surface ($\varepsilon = 1$) (a–d) and corresponding scattering indicatrices (e–h) for $H = 3$ and $\theta_i = 75^\circ$ (a and e), 45° (b and f), 15° (c and g), and 0 (d and h): the dotted curves show the Maxwellian distribution of the velocity component; the dashed curves show the cosine distribution.

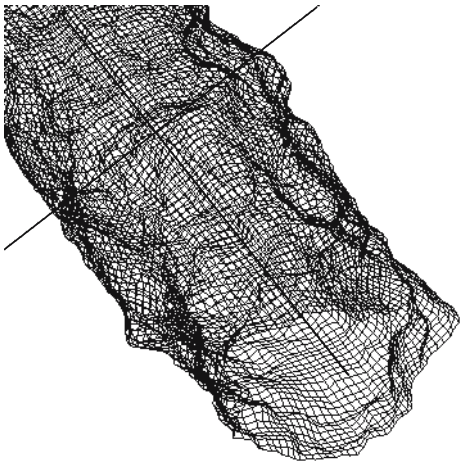

Fig. 4. Rough channel with $L/R = 6$ based on atomic-force microscopy data.

is necessary to choose the intersection point located most closely to the trajectory beginning point. Note that this procedure ensures 10-fold to 12-fold speedup of the search for the intersection point, as compared with consecutive checkup of each triangle for determining the possibility of intersection with the particle trajectory. After a collision with the surface, a new velocity vector is sampled in accordance with a specified interaction law. The procedure of particle motion lasts until the particle intersects the channel entrance or exit.

The particle passage probability w was estimated for cylindrical channels of three types: 1) channel whose structure was reconstructed in accordance with the data of atomic-force microscopy on the basis of the "experimental" surface (Fig. 4); 2) channel obtained by superposition of six "statistical" surfaces with the distribution function of microscopic roughness elements over the height close to the distribution function of the roughness of channel type 1 (Fig. 5); 3) channel with a regular structure of surface roughness (degenerate case) obtained by uniform distribution of identical peaks on the surface. All channels have an identical average height of the microscopic

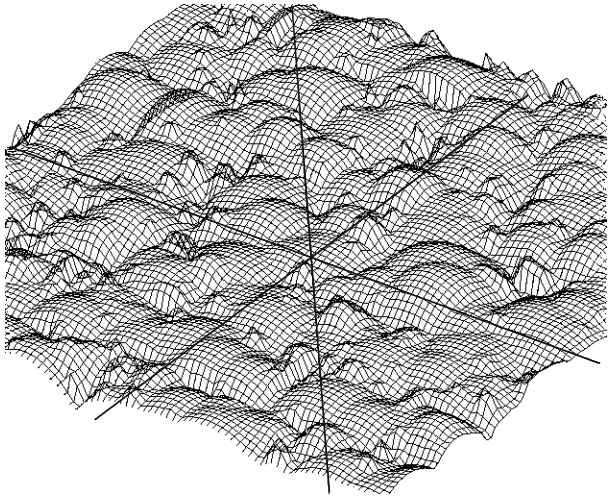

Fig. 5

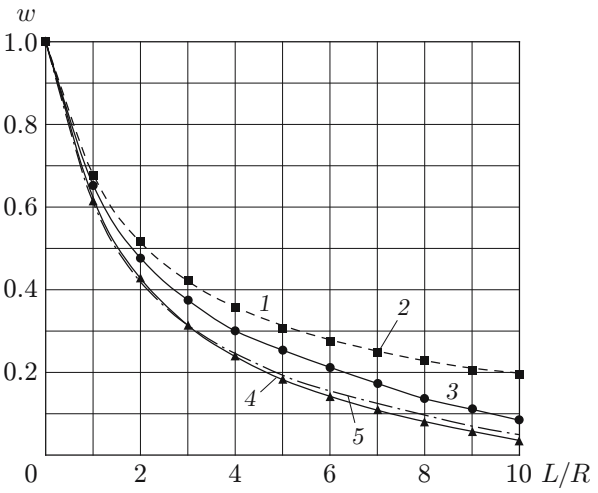

Fig. 6

Fig. 5. "Statistical" surface.

Fig. 6. Particle passage probability w in cylindrical channels: Clausing's data (1), "smooth" structure (2), "real" structure (3), "statistical" structure (4), and "regular" structure (5).

roughness elements $H_{\text{ave}} = 1.1$ μm. The ratio of the channel radius R to the average height of the microscopic surface roughness H_{ave} was changed in the simulations, while the channel length L remained constant. To check the correctness of the scheme developed, we performed a series of test computations to determine the particle passage probability in smooth cylindrical channels and compared the results of these test computations with the analytical data of Clausing [9]. Figure 6 shows the particle passage probability w obtained for different values of L/R for the channels described above. The results of the test computations are seen to be almost coincident with the data [9] in the entire range of L/R considered. Small differences are probably caused by the fact that the cross-sectional shape of the channel over its entire length is a broken circumference curved over the perimeter. Clausing [9] assumed the channel cross section to be a perfect circle. Some differences in data for the "statistical" and "regular" surface roughness for channels with $L/R < 4$ are caused by an insignificant effect of gas–surface interaction on the flow in comparatively short channels. At the same time, the results obtained for the channel surface simulated by statistical methods and for the "experimental" surface obtained from the data of atomic-force microscopy are noticeably different, though the surface structures have similar distribution functions of the roughness height in both cases. We can assume that the reason for this difference is the shape of individual microscopic roughness elements on the surfaces considered.

Thus, the average height of the microscopic roughness elements, like the distribution function of the roughness height, is not the only factor responsible for the characteristics of the free-molecular gas flow in a channel with rough walls.

Conclusions. The method developed allows one to construct a rough surface whose distribution function is almost coincident with the distribution function of the roughness height for the surface obtained with the use of atomic-force microscopy.

By modeling the scattering of molecular beams, the distribution function of particles reflected from the rough surface is obtained in an analytical form. This function can be used for specifying the boundary conditions for the gas-dynamic description of flow fields near the surface with a certain level of roughness.

An analysis of results of numerical simulations of the rarefied gas flow in a channel with allowance for the channel-surface structure shows that the surface roughness exerts a significant effect on the gas-dynamic conductivity of the channel in the entire range of the values of L/R considered.

It is demonstrated that the average height of the microscopic roughness element and the distribution function of the roughness height are not the only factors that affect the passage probability of gas molecules in a cylindrical channel.

REFERENCES

1. S. F. Borisov, "Progress in gas/surface interaction study," in: *Proc. of the 24th Int. Symp. on Rarefied Gas Dynamics*, (Monopoli, Bari, Italy, July 10–16, 2004), Vol. 762, Amer. Inst. of Phys., Mellville, New York (2005), pp. 933–940.
2. T. Sawada, B. Y. Horie, and W. Sugiyama, "Diffuse scattering of gas molecules from conical surface roughness," *J. Vacuum*, **47**, 795–797 (1996).
3. D. H. Davis, L. L. Levenson, and N. Milleron, "Effect of 'Rougher-than-Rough' surfaces on molecular flow through short ducts," *J. Appl. Phys.*, **35**, 529–532 (1964).
4. B. T. Porodnov, P. E. Suetin, S. F. Borisov, and V. D. Akinshin, "Experimental investigation of rarefied gas flow in different channels," *J. Fluid Mech.*, **64**, No. 3, 417–437 (1974).
5. O. E. Gerasimova, S. F. Borisov, C. Boragno, and U. Valbusa, "Modeling of the surface structure in gasdynamic problems with the use of the data of atomic force microscopy," *J. Eng. Phys. Thermophys.*, **76**, No. 2, 413–416 (2003).
6. O. A. Aksenova and I. A. Khalidov, "Fractal and statistical models of rough surface interacting with rarefied gas flow," in: *Proc. of the 24th Int. Symp. on Rarefied Gas Dynamics* (Monopoli, Bari, Italy, July 10–16, 2004), Vol. 762, Amer. Inst. of Phys., Mellville–New York (2005), pp. 993–998.
7. N. Gimelshein, J. Duncan, T. Lilly, et al., "Surface roughness effects in low Reynolds number channel flows," in: *Proc. of the 25th Int. Symp. on Rarefied Gas Dynamics* (St. Petersburg, Russia, July 21–28, 2006), Publ. House of the Sib. Branch of the Russian Acad. of Sci., Novosibirsk (2007), pp. 695–702.
8. G. A. Bird, *Molecular Gas Dynamics and the Direct Simulation of Gas Flows*, Oxford Univ. Press, New York (1994).
9. P. Clausing, "The flow of highly rarefied gases through tubes of arbitrary length," *J. Ann. Phys.*, **12**, 961–989 (1932).